Zeitschrift: IABSE publications = Mémoires AIPC = IVBH Abhandlungen
Band: 32 (1972)

Artikel: Finite element stability analysis of thin shells
Autor: Mathew, C.I.
DOI: https://doi.org/10.5169/seals-24956

Finite Element Stability Analysis of Thin Shells

Analyse de stabilité de coques minces au moyen de la méthode des éléments finis

Stabilitätsanalyse dünner Schalen mittels der endlichen Elemente-Methode

C. I. MATHEW
B.E., D.I.C., M.Sc. (Eng.) (Lond.), M.ASCE., Principal, Government Polytechnic, Kalamassery, Kerala, India

Introduction

Although the problem of elastic stability belongs inherently to the domain of nonlinear theory of elasticity, important results may be obtained from a linearized theory. The general theory assumes that the loads are conservative and the external loads on the structure are specified as the product of a unit load system and a single load parameter f. A potential energy then exists for the mechanical system consisting of the elastic structure and the external loads. The potential energy has a proper minimum in the stable part but only a stationary value in the unstable part. The critical point may now be characterised by a positive semi-definite second variation of the energy. Two types of singular behaviour due to the loss of stability may now occur characterised by the limit point or the bifurcation point.

Thus although all critical points are characterised by similar Eigenvalue problems, the actual behaviour of the structure at loads in the vicinity of the critical load may vary widely. For Example, flat plates can support loads in their plane far in excess of the critical load. On the other hand, some shell structures fail at loads which are only fraction of the critical loads predicted by the linear theory.

Basic Theory

In a mathematical sense, stability implies a configuration where infinitesimal disturbances will cause only infinitesimal departures from the given equilibrium configuration. In the system investigated here, it is assumed that the stresses

in the model subjected to a conservative set of inplane loads do not change during buckling deformation. This is consistent with the theory of elastic stability.

Thus if T represents the change in potential energy during the buckling deformation, we can write

$$T = U + V, \tag{1}$$

where U is the strain energy caused by the buckling deformation and V is the potential energy of the external loads measured from the unbuckled position.

For structural systems made up of linear elastic material, the change in potential energy T is a quadratic function of the generalised displacements that describe the buckled deformation. Since the first variation of T must vanish to satisfy equilibrium, a sufficient condition that T be a relative minimum is $T \geqq 0$ for all possible buckling deformation configurations. A criterion for determining the critical load can then be that $T = 0$ for some configuration. This is the familiar TIMOSHENKO [1] criterion for stability of elastic systems.

Let
$$U = \tfrac{1}{2} r^T K r \tag{2}$$

and
$$V = -\tfrac{1}{2} r^T f K_s r, \tag{3}$$

where r represents collectively the generalised nodal displacements, K is the flexural stiffness matrix of the model, and K_s is the stability matrix of the model.

Then
$$T = \tfrac{1}{2} r^T (K - f K_s) r = 0. \tag{4}$$

As $T = 0$ for $r \neq 0$, the matrix of the quadratic form $(K - f K_s)$ is positive semidefinite; therefore the critical load is obtained as the lowest root of the determinant equation

$$|K - f K_s| = 0. \tag{5}$$

Stiffness Matrix

The shell is considered as an assemblage of flat elements connected to each other at the nodal points. The stiffness matrix for the element is derived by allowing for three displacements and two rotations at each node.

For a typical rectangular element $ijkl$ shown in Fig. 1 the generalised displacements at the ith node are

$$d_i = \begin{Bmatrix} u_i \\ v_i \\ w_i \\ w_{i,y} \\ -w_{i,x} \end{Bmatrix}. \tag{6}$$

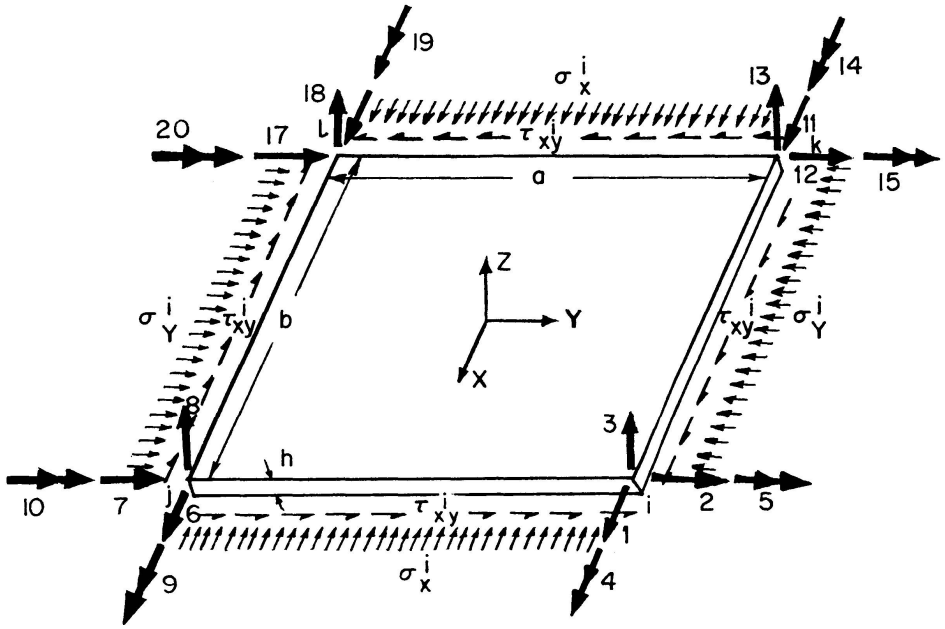

Fig. 1.

Here u_i, v_i, w_i are the displacements along the X, Y, Z directions respectively at the node i.

Selecting the MELOSH-ZIENKIEWICZ [2], [3] displacement functions we have,

$$\begin{aligned} u &= a_1 + a_2 x + a_3 y + a_4 x y, \\ v &= a_5 + a_6 x + a_7 y + a_8 x y, \\ w &= a_9 + a_{10} x + a_{11} y + a_{12} x^2 + a_{13} x y + a_{14} y^2 + a_{15} x^3 \\ &\quad + a_{16} x^2 y + a_{17} x y^2 + a_{18} y^3 + a_{19} x^3 y + a_{20} x y^3 . \end{aligned} \tag{7}$$

Here u, v, w describe displacements along X, Y, Z directions of a point (x, y) in the plate in terms of the constants Eq. (7) may now be written in short form as

$$\begin{Bmatrix} u \\ v \\ w \end{Bmatrix} = P a . \tag{8}$$

Here P is a 3×20 matrix in terms of the variables x, y. a is a 20×1 vector of constants $a_1 \ldots a_{20}$.

Considering all four nodes, the nodal deformation vector of the element is written in the matrix form as

$$r^e = G a . \tag{9}$$

Here, G is a 20×20 matrix in terms of the coordinates of the nodes, and r^e is a 20×1 vector of generalised displacements of the nodes of the element.

The unknown constants a are given by

$$a = G^{-1} r^e . \tag{10}$$

The generalised strains at any point is given by

$$e = \begin{Bmatrix} \dfrac{\partial u}{\partial x} \\ \dfrac{\partial v}{\partial y} \\ \dfrac{\partial u}{\partial y} + \dfrac{\partial v}{\partial x} \\ -\dfrac{\partial^2 w}{\partial x^2} \\ -\dfrac{\partial^2 w}{\partial y^2} \\ 2\dfrac{\partial^2 w}{\partial x\, \partial y} \end{Bmatrix} \tag{11}$$

or
$$e = C a = C G^{-1} r^e. \tag{12}$$

The stress at any point is given by

$$\sigma = D e = D C G^{-1} r^e. \tag{13}$$

For an isotropic material, the 6×6 matrix of elastic constants D is given by

$$D = \begin{bmatrix} D_1 & & & & & \\ D_1 & D_1 & & & & \\ 0 & 0 & (1-\mu) D_1/2 & & & \\ 0 & 0 & 0 & D_2 & & \\ 0 & 0 & 0 & D_2 & D_2 & \\ 0 & 0 & 0 & 0 & 0 & (1-\mu) D_2/2 \end{bmatrix}. \tag{14}$$

Here
$$D_1 = E h/(1-\mu^2);\ D_2 = E h^3/12(1-\mu^2),$$
E = Modulus of Elasticity,
μ = Poisson's Ratio,
h = Thickness of the plate element.

Now the strain energy of the element

$$U^e = \tfrac{1}{2} e^T D e\, dv,$$
$$= \tfrac{1}{2} r^{eT} G^{-1\,T} \int_v C^T D C\, dv\, G^{-1} r^e$$

or
$$U^e = \tfrac{1}{2} r^{eT} k^e r^e, \tag{15}$$

where
$$k^e = G^{-1\,T} \int_v C^T D C\, dv\, G^{-1} \tag{16}$$

represents the 20×20 stiffness matrix of the element.

The stiffness matrix of the element as obtained in Eq. (16) is with respect to the element co-ordinate axes $X Y Z$. This matrix is transformed into the

global co-ordinate system PQR to form the cylindrical shell element stiffness matrix k^s so that

$$k^s = T^T k^s T. \tag{17}$$

The 20×20 transformation matrix is given by

$$T = \begin{bmatrix} t_r & & & & \\ & t_1 & & 0 & \\ & & t_r & & \\ & 0 & & t_1 & \end{bmatrix} \tag{18}$$

and the 5×5 matrix t_1 is given by

$$t_1 = \begin{bmatrix} 1 & 0 & 0 & 0 & 0 \\ 0 & \operatorname{Cos} M & -\operatorname{Sin} M & 0 & 0 \\ 0 & \operatorname{Sin} M & \operatorname{Cos} M & 0 & 0 \\ 0 & 0 & 0 & 1 & 0 \\ 0 & 0 & 0 & 0 & \operatorname{Cos} M \end{bmatrix}. \tag{19}$$

The t_r matrix is obtained by substituting $-N$ for M in Eq. (19). The angles M and N are defined in Fig. 2. The stiffness matrix of the shell element is given in appendix 1.

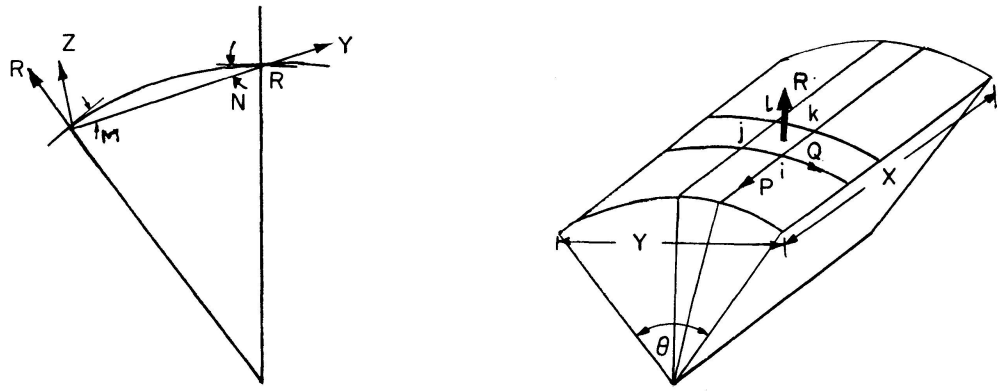

Fig. 2.

Stability Matrix

The potential energy of loads of the element shown in Fig. 1, measured from the unbuckled state is

$$V = -\frac{h}{2} \int_{-a/2}^{a/2} \int_{-b/2}^{b/2} \left[\sigma_x^i \left(\frac{\partial v}{\partial x} \right)^2 + \sigma_y^i \left(\frac{\partial u}{\partial y} \right)^2 + \sigma_x^i \left(\frac{\partial w}{\partial x} \right)^2 + \sigma_y^i \left(\frac{\partial w}{\partial y} \right)^2 + 2 \tau_{xy}^i \frac{\partial w}{\partial x} \frac{\partial w}{\partial y} \right] dx\, dy. \tag{20}$$

Here σ_x^i, and σ_y^i are the initial direct stresses in the x and y directions and τ_{xy}^i is the initial shear stress. In matrix form Eq. (20) may be written as

$$V = -\frac{h}{2}\int_{-a/2}^{a/2}\int_{-b/2}^{b/2} \begin{Bmatrix} \frac{\partial v}{\partial x} \\ \frac{\partial u}{\partial y} \\ \frac{\partial w}{\partial x} \\ \frac{\partial w}{\partial y} \end{Bmatrix}^T \begin{bmatrix} \sigma_x^i & 0 & 0 & 0 \\ 0 & \sigma_y^i & 0 & 0 \\ 0 & 0 & \sigma_x^i & \tau_{xy}^i \\ 0 & 0 & \tau_{xy}^i & \sigma_y^i \end{bmatrix} \begin{Bmatrix} \frac{\partial v}{\partial x} \\ \frac{\partial u}{\partial y} \\ \frac{\partial w}{\partial x} \\ \frac{\partial w}{\partial y} \end{Bmatrix} dx\,dy. \tag{21}$$

Now

$$\begin{Bmatrix} \frac{\partial v}{\partial x} \\ \frac{\partial u}{\partial y} \\ \frac{\partial w}{\partial x} \\ \frac{\partial w}{\partial y} \end{Bmatrix} = Ba = BG^{-1}r^e, \tag{22}$$

where B is a 4×20 matrix in variables x and y.

Thus Eq. (21) reduces to

$$V = -\frac{h}{2}\int_{-a/2}^{a/2}\int_{-b/2}^{b/2} r^{eT} G^{-1\,T} B^T \sigma^i B G^{-1} r^e\,dx\,dy. \tag{23}$$

Here σ^i is the initial stress matrix given in Eq. (21).

The stability matrix for the element is thus obtained as

$$k_s = -h\int_{-a/2}^{a/2}\int_{-b/2}^{b/2} G^{-1\,T} B^T \sigma^i B G^{-1}\,dx\,dy. \tag{24}$$

The reoriented shell element stability matrix is obtained by the same transformation used in the stiffness matrix. Thus

$$k_s^s = T^T k_s T.$$

For buckling under axial loads

$$\sigma_y^i = \tau_{xy}^i = 0.$$

The shell stability matrix under uniform axial compression for a rectangular element is given in appendix I.

Analysis

The general stiffness matrix K and the general stability matrix K_s are assembled using the code number technique [4]. The critical load is determined as the lowest Eigenvalue of the determinant Eq. (5). The standard computer program is capable of handling shells having various boundary conditions, varying thickness, openings and anisotropic material. Plate stability [5], [7] is only a special case of shell stability [6] problem in which M and N are zero.

To find the critical stress intensity on the structure, Eq. (5) is divided by f and brought to the form

$$\frac{1}{f} K r_i = K_s r, \tag{25}$$

in which both r_i and r represent the mode of the first buckling failure. An arbitrary normalised vector is assumed for r and r_i is determined. The coefficient $1/f$ of r_i when it is normalised represents the reciprocal of the first approximation of the lowest critical intensity. The normalised vector r_i thus found is used for r in Eq. (25) and the operation is repeated as the successive Eigenvalues converge. To facilitate faster convergence, and to determine the true mode shape a modification in the procedure is introduced, when two successive approximations of f come within about one percent.

The sought Eigenvalue f of Eq. (25) is replaced by

$$f = m f_1 + f_2, \tag{26}$$

where f_1 is the already found approximation, and m is the coefficient somewhat smaller than unity, such as 0.9, and f_2 – the required addition to be found.

Eq. (25) is then brought to the form,

$$\frac{1}{f_2} (K - m f_1 K_s) r_i = K_s r. \tag{27}$$

The matrix $(K - m f_1 K_s)$ is known and Eq. (27) is solved for f_2 to the required accuracy in the way, in which the Eq. (25) has just been used. The mode of failure is described closely by the eigen vector r_i found from Eq. (27). The subsequent eigenvalues may be found by the same procedure after sweeping the eigen-vectors found from the trial vector r.

The critical loads of curved panels and cylindrical shells simply supported on all edges under uniform axial compression are determined and are compared with the theoretical results [1]. In all the examples the Young's Modulus is unity and Poisson's ratio 1/3.

The critical loads of curved panels $12'' \times 12'' \times 1''$ subtending angles 0° (plate), 10°, 20°, and 30° at centre, simply supported on all edges, for various element sizes are tabulated in Table 1. The critical load of a cylindrical shell

is determined by analysing a 90° sector of the shell with appropriate boundary conditions. Table 2 gives the critical load on a shell simply supported on both edges. The sector has a height of 12″, thickness of 1″, and a quadrant length of 54″. In general the values obtained by the finite element method show good agreement with the existing theoretical results.

Cylindrical shells of medium length under axial compression have a large number of simultaneous buckling modes. Table 3 which gives the first five Eigenvalues of a matrix of order 383 and half band width 31, illustrates the effectiveness of the method adopted to isolate the close Eigenvalues. Analysis of a 90° sector of a simply supported shell with 36×8 elements involved a matrix of order 1485 and half band width of 51. A similar shell with 18×12 elements involved a matrix of order and half band width 1111×71. The critical load in each case was determined in about 450 seconds on IBM 360.

Table 1. Unit Stress at Critical Load

Elements	0°	10°	20°	30°
3×3	0.023065	0.023775	0.025894	0.029388
4×4	0.024120	0.024805	0.026850	0.030234
6×6	0.024947	0.025623	0.027610	0.030910
8×8	0.025267	0.025933	0.027900	0.031177
Elastic Solution	0.025702	0.026373	0.028755	0.032646

Table 2. Unit Stress at Critical Load

Elements	90° Shell $54'' \times 12'' \times 1''$
2×9	0.015658
4×18	0.017085
8×36	0.017503
Elastic Solution	0.017813

Table 3. Eigenvalues 90° Shell $54'' \times 12'' \times 1''$ 4×18 Elements

1	0.017085
2	0.017474
3	0.018425
4	0.022983
5	0.028683

Table 4. Unit Stress at Critical Load

Full Circle Solution	90° Shell $72'' \times 96'' \times 1''$	90° Shell $72'' \times 48'' \times 1''$
Fixed at both Ends	0.012858	0.013467
Simply supported at both ends	0.012561	0.012561
Elastic Solution Simply supported Shell	0.013359	0.013359

The effect of edge conditions on the critical load was also studied by doubling the length of the shell. Table 4 indicates that the critical load of a shell of length equal to its diameter, is that of a simply supported shell irrespective of the boundary conditions.

Conclusions

1. Finite element solutions on subdivision of elements converge monotonically to the theoretical values providing a lowerbound on the theoretical solutions.

2. The results confirm the general validity of the finite element technique in problems of buckling of cylindrical shells.

3. The usefulness of the method lies largely in its applicability to problems for which theoretical solutions are not available. The finite element method overcomes the problem of irregular boundary conditions, nonuniform thickness, segmentation of shells and openings in the shell.

4. To obtain meaningful results, the model should have sufficient number of elements to describe the buckling mode. Thus any shell buckling problem involves determination of Eigenvalues of large matrices. This is overcome by the new method devised in the paper.

5. The presence of imperfections in the shape and properties of the shell make the theory inapplicable.

Acknowledgements

The invaluable assistance of Dr. A. Hrennikoff, Professor Emeritus, University of British Columbia, Vancouver, and the free computer facilities received from the university of British Columbia computing center are gratefully acknowledged.

Appendix I

Table 5 gives the 20×20 stiffness, or stability matrix for a general rectangular cylindrical shell element. Entries of the stiffness matrix are obtained by substituting Table 6 in Table 5 and those of the stability matrix by substituting Table 7 in Table 5.

Table 5

Symmetrical

	1	2	3	4	5
1	X_{11}				
2	$Y_{11}\,\mathrm{Cos}\,N$	$Y_{12}\,\mathrm{Cos}^2 N + F_{13}\,\mathrm{Sin}^2 N$			
3	$Y_{11}\,\mathrm{Sin}\,N$	$(Y_{12}-F_{13})\,\mathrm{Cos}\,N \cdot \mathrm{Sin}\,N$	$Y_{12}\,\mathrm{Sin}^2 N + F_{13}\,\mathrm{Cos}^2 N$		
4	—	$-m^x_{13}\,\mathrm{Sin}\,N$	$m^x_{13}\,\mathrm{Cos}\,N$	m^x_{14}	
5	—	$-m^y_{13}\,\mathrm{Cos}\,N\,\mathrm{Sin}\,N$	$m^y_{13}\,\mathrm{Cos}^2 N$	$m^y_{14}\,\mathrm{Cos}\,N$	$m^y_{15}\,\mathrm{Cos}^2 N$
6	X_{21}	$X_{22}\,\mathrm{Cos}\,N$	$X_{22}\,\mathrm{Sin}\,N$	—	—
7	$Y_{21}\,\mathrm{Cos}\,M$	$Y_{22}\,\mathrm{Cos}\,N\,\mathrm{Cos}\,M - F_{23}\,\mathrm{Sin}\,N\,\mathrm{Sin}\,M$	$Y_{22}\,\mathrm{Cos}\,M\,\mathrm{Sin}\,N + F_{23}\,\mathrm{Cos}\,N\,\mathrm{Sin}\,M$	$F_{24}\,\mathrm{Sin}\,M$	$F_{25}\,\mathrm{Cos}\,N\,\mathrm{Sin}\,M$
8	$-Y_{21}\,\mathrm{Sin}\,M$	$-Y_{22}\,\mathrm{Cos}\,N\,\mathrm{Sin}\,M - F_{23}\,\mathrm{Cos}\,M\,\mathrm{Sin}\,N$	$-Y_{22}\,\mathrm{Sin}\,N\,\mathrm{Sin}\,M + F_{23}\,\mathrm{Cos}\,N\,\mathrm{Cos}\,M$	$F_{24}\,\mathrm{Cos}\,N$	$F_{25}\,\mathrm{Cos}\,N\,\mathrm{Cos}\,M$
9	—	$-m^x_{23}\,\mathrm{Sin}\,N$	$m^x_{23}\,\mathrm{Cos}\,N$	m^x_{24}	$m^x_{25}\,\mathrm{Cos}\,N$
10	—	$-m^y_{23}\,\mathrm{Cos}\,M\,\mathrm{Sin}\,N$	$m^y_{23}\,\mathrm{Cos}\,N\,\mathrm{Cos}\,M$	$m^y_{24}\,\mathrm{Cos}\,M$	$m^y_{25}\,\mathrm{Cos}\,N\,\mathrm{Cos}\,M$
11	X_{31}	$X_{32}\,\mathrm{Cos}\,N$	$X_{32}\,\mathrm{Sin}\,N$	—	—
12	$Y_{31}\,\mathrm{Cos}\,N$	$Y_{32}\,\mathrm{Cos}^2 N + F_{33}\,\mathrm{Sin}^2 N$	$(Y_{32}-F_{33})\,\mathrm{Cos}\,N \cdot \mathrm{Sin}\,N$	$-F_{34}\,\mathrm{Sin}\,N$	$-F_{35}\,\mathrm{Cos}\,N\,\mathrm{Sin}\,N$
13	$Y_{31}\,\mathrm{Sin}\,N$	$(Y_{32}-F_{33})\,\mathrm{Cos}\,N \cdot \mathrm{Sin}\,N$	$Y_{32}\,\mathrm{Sin}^2 N + F_{33}\,\mathrm{Cos}^2 N$	$F_{34}\,\mathrm{Cos}\,N$	$F_{35}\,\mathrm{Cos}^2 N$
14	—	$-m^x_{33}\,\mathrm{Sin}\,N$	$m^x_{33}\,\mathrm{Cos}\,N$	m^x_{34}	$m^x_{35}\,\mathrm{Cos}\,N$
15	—	$-m^y_{33}\,\mathrm{Cos}\,N\,\mathrm{Sin}\,N$	$m^y_{33}\,\mathrm{Cos}^2 N$	$m^y_{34}\,\mathrm{Cos}\,N$	$m^y_{35}\,\mathrm{Cos}^2 N$
16	X_{41}	$X_{42}\,\mathrm{Cos}\,N$	$X_{42}\,\mathrm{Sin}\,N$	—	—
17	$Y_{41}\,\mathrm{Cos}\,M$	$Y_{42}\,\mathrm{Cos}\,N\,\mathrm{Cos}\,M - F_{43}\,\mathrm{Sin}\,N\,\mathrm{Sin}\,M$	$Y_{42}\,\mathrm{Cos}\,M\,\mathrm{Sin}\,N + F_{43}\,\mathrm{Cos}\,N\,\mathrm{Sin}\,M$	$F_{44}\,\mathrm{Sin}\,M$	$F_{45}\,\mathrm{Cos}\,N\,\mathrm{Sin}\,M$
18	$-Y_{41}\,\mathrm{Sin}\,M$	$-Y_{42}\,\mathrm{Cos}\,N\,\mathrm{Sin}\,M - F_{43}\,\mathrm{Cos}\,M\,\mathrm{Sin}\,N$	$-Y_{42}\,\mathrm{Sin}\,N\,\mathrm{Sin}\,M + F_{43}\,\mathrm{Cos}\,N\,\mathrm{Cos}\,M$	$F_{44}\,\mathrm{Cos}\,M$	$F_{45}\,\mathrm{Cos}\,N\,\mathrm{Cos}\,M$
19	—	$-m^x_{43}\,\mathrm{Sin}\,N$	$m^x_{43}\,\mathrm{Cos}\,N$	m^x_{44}	$m^x_{45}\,\mathrm{Cos}\,N$
20	—	$-m^y_{43}\,\mathrm{Cos}\,M\,\mathrm{Sin}\,N$	$m^y_{43}\,\mathrm{Cos}\,N\,\mathrm{Cos}\,M$	$m^y_{44}\,\mathrm{Cos}\,M$	$m^y_{45}\,\mathrm{Cos}\,N\,\mathrm{Cos}\,M$

6	X_{11}				
7	$-Y_{11}\,\mathrm{Cos}\,M$	$Y_{12}\,\mathrm{Cos}^2 M + F_{13}\,\mathrm{Sin}^2 M$	Symmetrical		
8	$Y_{11}\,\mathrm{Sin}\,M$	$(F_{13}-Y_{12})\,\mathrm{Cos}\,M \cdot \mathrm{Sin}\,M$	$Y_{12}\,\mathrm{Sin}^2 M + F_{13}\,\mathrm{Cos}^2 M$		
9	—	$-m^x_{13}\,\mathrm{Sin}\,M$	$-m^x_{13}\,\mathrm{Cos}\,M$	m^x_{14}	
10	—	$m^y_{13}\,\mathrm{Cos}\,M\,\mathrm{Sin}\,M$	$m^y_{13}\,\mathrm{Cos}^2 M$	$-m^y_{14}\,\mathrm{Cos}\,M$	$m^y_{15}\,\mathrm{Cos}^2 M$
11	X_{41}	$-X_{42}\,\mathrm{Cos}\,M$	$X_{42}\,\mathrm{Sin}\,M$	—	—
12	$-Y_{41}\,\mathrm{Cos}\,N$	$Y_{42}\,\mathrm{Cos}\,N\,\mathrm{Cos}\,M - F_{43}\,\mathrm{Sin}\,N\,\mathrm{Sin}\,M$	$-Y_{42}\,\mathrm{Cos}\,N\,\mathrm{Sin}\,M - F_{43}\,\mathrm{Cos}\,M\,\mathrm{Sin}\,N$	$F_{44}\,\mathrm{Sin}\,N$	$-F_{45}\,\mathrm{Cos}\,M\,\mathrm{Sin}\,N$
13	$-Y_{41}\,\mathrm{Sin}\,N$	$Y_{42}\,\mathrm{Cos}\,M\,\mathrm{Sin}\,N + F_{43}\,\mathrm{Cos}\,N\,\mathrm{Sin}\,M$	$-Y_{42}\,\mathrm{Sin}\,N\,\mathrm{Sin}\,M + F_{43}\,\mathrm{Cos}\,N\,\mathrm{Cos}\,M$	$-F_{44}\,\mathrm{Cos}\,N$	$F_{45}\,\mathrm{Cos}\,N\,\mathrm{Cos}\,M$
14	—	$-m^x_{43}\,\mathrm{Sin}\,M$	$-m^x_{43}\,\mathrm{Cos}\,M$	m^x_{44}	$-m^x_{45}\,\mathrm{Cos}\,M$
15	—	$m^y_{43}\,\mathrm{Cos}\,N\,\mathrm{Sin}\,M$	$m^y_{43}\,\mathrm{Cos}\,N\,\mathrm{Cos}\,M$	$-m^y_{44}\,\mathrm{Cos}\,N$	$m^y_{45}\,\mathrm{Cos}\,N\,\mathrm{Cos}\,M$
16	X_{31}	$-X_{32}\,\mathrm{Cos}\,M$	$X_{32}\,\mathrm{Sin}\,M$	—	—
17	$-Y_{31}\,\mathrm{Cos}\,M$	$Y_{32}\,\mathrm{Cos}^2 M + F_{33}\,\mathrm{Sin}^2 M$	$(F_{33}-Y_{32})\,\mathrm{Cos}\,M \cdot \mathrm{Sin}\,M$	$-F_{34}\,\mathrm{Sin}\,M$	$F_{35}\,\mathrm{Cos}\,M\,\mathrm{Sin}\,M$
18	$Y_{31}\,\mathrm{Sin}\,M$	$(F_{33}-Y_{32})\,\mathrm{Cos}\,M \cdot \mathrm{Sin}\,M$	$Y_{32}\,\mathrm{Sin}^2 M + F_{33}\,\mathrm{Cos}^2 M$	$-F_{34}\,\mathrm{Cos}\,M$	$F_{35}\,\mathrm{Cos}^2 M$
19	—	$-m^x_{33}\,\mathrm{Sin}\,M$	$-m^x_{33}\,\mathrm{Cos}\,M$	m^x_{34}	$-m^x_{35}\,\mathrm{Cos}\,M$
20	—	$m^y_{33}\,\mathrm{Cos}\,M\,\mathrm{Sin}\,M$	$m^y_{33}\,\mathrm{Cos}^2 M$	$-m^y_{34}\,\mathrm{Cos}\,M$	$m^y_{35}\,\mathrm{Cos}^2 M$
	6	7	8	9	10

11	X_{11}				
12	$-Y_{11}\ \mathrm{Cos}\ N$	$Y_{12}\ \mathrm{Cos}^2\ N$ $+F_{13}\ \mathrm{Sin}^2\ N$	Symmetrical		
13	$-Y_{11}\ \mathrm{Sin}\ N$	$(Y_{12}-F_{13})\ \mathrm{Cos}\ N$ $\cdot \mathrm{Sin}\ N$	$Y_{12}\ \mathrm{Sin}^2\ N$ $+F_{13}\ \mathrm{Cos}^2\ N$		
14	—	$-m^x_{13}\ \mathrm{Sin}\ N$	$m^x_{13}\ \mathrm{Cos}\ N$	m^x_{14}	
15	—	$m^y_{13}\ \mathrm{Cos}\ N\ \mathrm{Sin}\ N$	$-m^y_{13}\ \mathrm{Cos}^2\ N$	$-m^y_{14}\ \mathrm{Cos}\ N$	$m^y_{15}\ \mathrm{Cos}^2\ N$
16	X_{21}	$-X_{22}\ \mathrm{Cos}\ N$	$-X_{22}\ \mathrm{Sin}\ N$	—	—
17	$-Y_{21}\ \mathrm{Cos}\ M$	$Y_{22}\ \mathrm{Cos}\ N\ \mathrm{Cos}\ M$ $-F_{23}\ \mathrm{Sin}\ N\ \mathrm{Sin}\ M$	$Y_{22}\ \mathrm{Cos}\ M\ \mathrm{Sin}\ N$ $+F_{23}\ \mathrm{Cos}\ N\ \mathrm{Sin}\ M$	$F_{24}\ \mathrm{Sin}\ M$	$-F_{25}\ \mathrm{Cos}\ N\ \mathrm{Sin}\ M$
18	$Y_{21}\ \mathrm{Sin}\ M$	$-Y_{22}\ \mathrm{Cos}\ N\ \mathrm{Sin}\ M$ $-F_{23}\ \mathrm{Cos}\ M\ \mathrm{Sin}\ N$	$-Y_{22}\ \mathrm{Sin}\ N\ \mathrm{Sin}\ M$ $+F_{23}\ \mathrm{Cos}\ N\ \mathrm{Cos}\ M$	$F_{24}\ \mathrm{Cos}\ M$	$-F_{25}\ \mathrm{Cos}\ N\ \mathrm{Cos}\ M$
19	—	$-m^x_{23}\ \mathrm{Sin}\ N$	$m^x_{23}\ \mathrm{Cos}\ N$	m^x_{24}	$-m^x_{25}\ \mathrm{Cos}\ N$
20	—	$m^y_{23}\ \mathrm{Cos}\ M\ \mathrm{Sin}\ N$	$-m^y_{23}\ \mathrm{Cos}\ N\ \mathrm{Cos}\ M$	$-m^y_{24}\ \mathrm{Cos}\ M$	$m^y_{25}\ \mathrm{Cos}\ N\ \mathrm{Cos}\ M$
	11	12	13	14	15

16	X_{11}				
17	$X_{11}\ \mathrm{Cos}\ M$	$Y_{12}\ \mathrm{Cos}^2\ M$ $+F_{13}\ \mathrm{Sin}^2\ M$	Symmetrical		
18	$-Y_{11}\ \mathrm{Sin\ M}$	$(F_{13}-Y_{12})\ \mathrm{Cos}\ M$ $\cdot \mathrm{Sin}\ M$	$Y_{12}\ \mathrm{Sin}^2\ M$ $+F_{13}\ \mathrm{Cos}^2\ M$		
19	—	$-m^x_{13}\ \mathrm{Sin}\ M$	$-m^x_{13}\ \mathrm{Cos}\ M$	m^x_{14}	
20	—	$-m^y_{13}\ \mathrm{Cos}\ M\ \mathrm{Sin}\ M$	$-m^y_{13}\ \mathrm{Cos}^2\ M$	$m^y_{14}\ \mathrm{Cos}\ M$	$m^y_{15}\ \mathrm{Cos}^2\ M$
	16	17	18	19	20

Table 6

The substitution of the following values in Table 5 will yield cylindrical shell element stiffness matrix.

$$F_{13} = (4k^4+4+2.8k^2-0.8\mu k^2)\, L/a\, k^3$$
$$F_{23} = (-4k^4+2-2.8k^2+0.8\mu k^2)\, L/a\, k^3$$
$$F_{33} = (2k^4-4-2.8k^2+0.8\mu k^2)\, L/a\, k^3$$
$$F_{43} = (-2k^4-2+2.8k^2-0.8\mu k^2)\, L/a\, k^3$$
$$F_{24} = (2k^2+0.2-0.2\mu)\, L/k$$
$$F_{34} = (-k^2+0.2+0.8\mu)\, L/k$$
$$F_{44} = (k^2-0.2+0.2\mu)\, L/k$$
$$F_{25} = (1-0.2k^2-0.8\mu k^2)\, L/k^2$$
$$F_{35} = (-2-0.2k^2+0.2\mu k^2)\, L/k^2$$
$$F_{45} = (-1+0.2k^2-0.2\mu k^2)\, L/k^2$$

$$m^x_{13} = (-2k^2-0.2-0.8\mu)\, L/k \qquad m^y_{13} = (2/k^2+0.2+0.8\mu)\, L$$
$$m^x_{23} = (-2k^2-0.2+0.2\mu)\, L/k \qquad m^y_{23} = (1/k^2-0.2-0.8\mu)\, L$$
$$m^x_{33} = (-k^2+0.2+0.8\mu)\, L/k \qquad m^y_{33} = (2/k^2+0.2-0.2\mu)\, L$$
$$m^x_{43} = (-k^2+0.2-0.2\mu)\, L/k \qquad m^y_{43} = (1/k^2-0.2+0.2\mu)\, L$$
$$m^x_{14} = (4-4\mu+20k^2)\, a\, L/15\, k \qquad m^y_{14} = -\mu\, a\, L$$
$$m^x_{24} = (-1+\mu+10k^2)\, a\, L/15\, k \qquad m^y_{24} = 0$$
$$m^x_{34} = (-4+4\mu+10k^2)\, a\, L/15\, k \qquad m^y_{34} = 0$$
$$m^x_{44} = (1-\mu+5k^2)\, a\, L/15\, k \qquad m^y_{44} = 0$$
$$m^y_{15} = (20+4k^2-4\mu k^2)\, a\, L/15\, k$$
$$m^x_{25} = 0 \qquad m^y_{25} = (10-4k^2+4\mu k^2)\, a\, L/15\, k$$
$$m^x_{35} = 0 \qquad m^y_{35} = (10-k^2+\mu k^2)\, a\, L/15\, k$$
$$m^x_{45} = 0 \qquad m^y_{45} = (5+k^2-\mu k^2)\, a\, L/15\, k$$

$$X_{11} = \left[\frac{1}{3k}+\frac{(1-\mu)k}{6}\right] D_1 \quad : \quad Y_{11} = \left[\frac{\mu}{4}+\frac{(1-\mu)}{8}\right] D_1$$
$$X_{21} = \left[\frac{1}{6k}-\frac{(1-\mu)k}{6}\right] D_1 \quad : \quad Y_{21} = \left[-\frac{\mu}{4}+\frac{(1-\mu)}{8}\right] D_1$$
$$X_{31} = \left[-\frac{1}{3k}+\frac{(1-\mu)k}{12}\right] D_1 : \quad Y_{31} = -Y_{21}$$
$$X_{41} = \left[-\frac{1}{6k}-\frac{(1-\mu)k}{12}\right] D_1 : \quad Y_{41} = -Y_{11}$$
$$X_{12} = Y_{11} \quad : \quad Y_{12} = \left[\frac{k}{3}+\frac{(1-\mu)}{6k}\right] D_1$$
$$X_{22} = -Y_{21} \quad : \quad Y_{22} = \left[-\frac{k}{3}+\frac{(1-\mu)}{12k}\right] D_1$$
$$X_{32} = Y_{21} \quad : \quad Y_{32} = \left[\frac{k}{6}-\frac{(1-\mu)}{6k}\right] D_1$$
$$X_{42} = -Y_{21} \quad : \quad Y_{42} = \left[-\frac{k}{6}-\frac{(1-\mu)}{12k}\right] D_1$$

Here,
$D_1 = E\,h/(1-\mu^2)$ — $k = b/a$, ratio of the sides
$D_2 = E\,h^3/12\,(1-\mu^2)$ — $L = D_2/a$
μ = Poisson's ratio — a = Length of Element along the "Y" axis
E = Young's modulus — b = Length of Element along the "X" axis
h = Thickness of the shell

Table 7

$X_{11} = 0$

$Y_{11} = 0$

$X_{21} = 0$

$Y_{21} = 0$

$X_{31} = 0$

$Y_{31} = -Y_{21}$

$X_{41} = 0$

$Y_{41} = -Y_{11}$

$Y_{12} = \dfrac{a\,h}{6\,b}\,\sigma_x^i$

$X_{22} = -Y_{21}$

$Y_{22} = \dfrac{a\,h}{12\,b}\,\sigma_x^i$

$X_{32} = Y_{21}$

$Y_{32} = -\dfrac{a\,h}{6\,b}\,\sigma_x^i$

$X_{42} = -Y_{11}$

$Y_{42} = -\dfrac{a\,h}{12\,b}\,\sigma_x^i$

$F_{13} = 276\,A$

$m_{13}^x = -33\,a\,A$

$m_{13}^y = 21\,b\,A$

$F_{23} = 102\,A$

$m_{23}^x = 19.5\,a\,A$

$m_{23}^y = 10.5\,b\,A$

$F_{33} = -276\,A$

$m_{33}^x = 33\,a\,A$

$m_{33}^y = 21\,b\,A$

$F_{43} = -102\,A$

$m_{43}^x = -19.5\,a\,A$

$m_{43}^y = 10.5\,b\,A$

$m_{14}^x = 6\,a^2\,A$

$m_{14}^y = 0$

$F_{24} = -19.5\,a\,A$

$m_{24}^x = -4.5\,a^2\,A$

$m_{24}^y = 0$

$F_{34} = 33\,a\,A$

$m_{34}^x = -6\,a^2\,A$

$m_{34}^y = 0$

$F_{44} = 19.5\,a\,A$

$m_{44}^x = 4.5\,a^2\,A$

$m_{44}^y = 0$

$m_{15}^y = 28\,b^2\,A$

$F_{25} = 10.5\,b\,A$

$m_{25}^x = 0$

$m_{25}^y = 14\,b^2\,A$

$F_{35} = -21\,b\,A$

$m_{35}^x = 0$

$m_{35}^y = -7\,b^2\,A$

$F_{45} = -10.5\,b\,A$

$m_{45}^x = 0$

$m_{45}^y = -3.5\,b^2\,A$

Here $A = \dfrac{h\,a\,\sigma_x^i}{630\,b}$

References

1. TIMOSHENKO, S.: Theory of Elastic stability. McGraw-Hill Book Co., Inc., New York, 1936.
2. MELOSH, R. J.: Basis for Derivation of Matrices for the Direct Stiffness Method. AIAA Journal, Vol. 1, July 1963, pp. 1631–1637.
3. ZIENKIEWICZ, O.C. and CHEUNG, Y. K.: The Finite Element Method in structural and continuum mechanics. McGraw-Hill, 1967.
4. TEZCAN, S. S.: Discussion of Simplified Formulation of Stiffness Matrices by Peter M. Wright, proceedings, paper 3478, April 1963, Journal of Structural Division, ASCE, Dec. 1963, pp. 445–449.
5. KAPUR, K. K. and HARTZ, B. J.: Stability of Plates using the Finite Element Method. Journal of the Engineering Mechanics Division ASCE. April 1966, pp. 177–195.
6. GALLAGHER, R. H., GELLATLY, R. A., PADLOG, J., and MALLET, R. H.: A Discrete Element. Procedure of Thin-Shell Instability Analysis. AIAA Journal, Vol. 5. January 1967, pp. 138–145.
7. HRENNIKOFF, A., MATHEW, C. I., and RAJAN SEN: Stability of Plates Using Rectangular Bar Cells. Publication pending by I.A.B.S.E.

Summary

This paper presents the finite element matrix displacement approach to the stability analysis of shells in general, and to the cylindrical shells in particular. The buckling of deep cylindrical shells is herein investigated considering the membrane and flexural stiffnesses. The stiffness and stability matrices for a rectangular shell element are presented in an explicit form. The critical loads of cylindrical shells have herein been determined using sophisticated Eigenvalue programs. The results obtained are compared with the theoretical solutions to demonstrate the convergence characteristics.

Résumé

Ce travail présente la méthode de la matrice de déplacements basée sur les éléments finis pour l'analyse de stabilité de coques en général et de coques cylindriques minces en particulier. Le voilement de coques cylindriques minces est examiné en tenant compte des rigidités de la membrane et à la flexion. Les matrices de rigidité et de stabilité pour un élément de coque rectangulaire sont présentées en forme explicite. Les charges critiques de coques cylindriques ont été déterminées en utilisant des programmes compliqués de valeurs propres. Les résultats obtenus sont comparés aux solutions théoriques pour en démontrer les caractéristiques concordantes.

Zusammenfassung

Die vorliegende Arbeit befasst sich mit der endlichen Elemente-Matrix-Verschiebungsnäherung zur Stabilitätsanalyse von Schalen im allgemeinen und von zylindrischen Schalen im besonderen. Die Beulung tiefer zylindrischer Schalen ist hierbei inbegriffen, unter Berücksichtigung der Membran- und Biegesteifigkeiten. Die Steifigkeits- und Stabilitätsmatrizen für ein rechteckiges Schalenelement werden in expliziter Form dargelegt. Die kritischen Belastungen zylindrischer Schalen wurden unter Benutzung komplexer Eigenwertprogramme bestimmt. Die erhaltenen Resultate werden mit den theoretischen Lösungen zum Zwecke der Übereinstimmung verglichen.